Vasostatin, a Calreticulin Fragment, Inhibits Angiogenesis and Suppresses Tumor Growth

By Sandra E. Pike,* Lei Yao,* Karen D. Jones,* Barry Cherney,* Ettore Appella,‡ Kazuyasu Sakaguchi,‡ Hira Nakhasi,* Julie Teruya-Feldstein,§ Peter Wirth,‖ Ghanshyam Gupta,* and Giovanna Tosato*

*From the *Center for Biologics Evaluation and Research, Rockville, Maryland 20852; and the ‡Laboratory of Cell Biology, the §Laboratory of Pathology, and the ‖Laboratory of Experimental Carcinogenesis, National Cancer Institute, Bethesda, Maryland 20892*

Summary

An endothelial cell inhibitor was purified from supernatant of an Epstein-Barr virus–immortalized cell line and identified as fragments of calreticulin. The purified recombinant NH_2-terminal domain of calreticulin (amino acids 1–180) inhibited the proliferation of endothelial cells, but not cells of other lineages, and suppressed angiogenesis in vivo. We have named this NH_2-terminal domain of calreticulin vasostatin. When inoculated into athymic mice, vasostatin significantly reduced growth of human Burkitt lymphoma and human colon carcinoma. Compared with other inhibitors of angiogenesis, vasostatin is a small, soluble, and stable molecule that is easy to produce and deliver. As an angiogenesis inhibitor that specifically targets proliferating endothelial cells, vasostatin has a unique potential for cancer treatment.

Key words: endothelial cells • angiogenesis • cell growth • cancer • antitumor agent

Tumor growth and invasion into normal tissues are dependent upon an adequate blood supply (1, 2). Agents that reduce tumor blood supply prevent or delay tumor formation, and promote the regression or dormancy of established tumors. Antibodies against vascular endothelial growth factor (VEGF),[1] which is produced at high levels by various types of tumors, antibodies against VEGF receptor 2, and soluble VEGF receptors reduced tumor growth in experimental animal models (3–5). Antibodies to the integrin $\alpha_v\beta_3$, which is expressed at high levels by angiogenic blood vessels and permits endothelial cells to interact with components of the extracellular matrix, disrupted ongoing angiogenesis on the chick chorioallantoid membrane and led to the regression of human tumors transplanted into this site (6–8). Both angiostatin, a fragment of plasminogen (9, 10), and endostatin, a fragment of collagen XVIII (11, 12), suppressed neovascularization and inhibited the growth of a variety of experimental tumors. IL-12 (13), the IFN-γ inducible protein-10 (IP-10; 14, 15), the monokine induced by INF-γ (Mig; 16, 17), a fragment of prolactin (18), synthetic analogues of fumagillin (19), thalidomide (20), platelet factor-4 (21), and thrombospondin (22) are multifunctional compounds that inhibited angiogenesis and exerted antitumor effects.

EBV-immortalized cell lines, which are usually not tumorigenic in athymic mice, can promote regression of experimental Burkitt lymphoma, colon carcinoma, and other human malignancies established in athymic mice through a vascular-based process (23, 24). The murine chemokines IP-10 and Mig, which are induced in the host by EBV-immortalized cells, can inhibit angiogenesis and contribute to tumor regression in this model (14, 15, 17). However, the participation of additional factors was suggested by the failure of IP-10 and Mig to promote complete tumor regression that is typically induced by EBV-immortalized cells. A role for factors released by EBV-immortalized cells was suggested by the observation that conditioned medium from these cells reduced tumor growth. We sought to identify factors secreted by EBV-immortalized cells that might directly inhibit angiogenesis and tumor growth.

Materials and Methods

Purification of Inhibitory Factor from Conditioned Medium. For production of conditioned medium, exponentially growing VDS-O cells (15) were washed free of serum and cultured (2.0×10^6

[1]*Abbreviations used in this paper:* aa, amino acids; bFGF, basic fibroblast growth factor; FBHE, fetal bovine heart endothelial cells; HUVEC, human umbilical vein endothelial cells; IP-10, IFN-γ inducible protein-10; MBP, maltose-binding protein; Mig, monokine induced by IFN-γ; VEGF, vascular endothelial growth factor.

S.E. Pike and L. Yao contributed equally to this work.

cells/ml) for 48 h in protein-free hybridoma medium–11 (GIBCO BRL, Gaithersburg, MD) supplemented with 5 μg/ml gentamicin (Sigma Chemical Co., St. Louis, MO). Cells and debris were removed by centrifugation and sterile filtration (0.45-μm filters), and 6.0 μg/ml Aprotinin (Sigma Chemical Co.) was added. After adsorption of nonpolar substances by addition of silica gel 60 (5 g/liter, EM Science, Gibbstown, NJ), the conditioned medium was filtered, concentrated 15-fold, and exchanged into 10 mM Na_2HPO_4/NaH_2PO_4, 100 mM NaCl, 0.1 mM imidazole (Sigma Chemical Co.), pH 8.3. The material was applied to a Chelating Sepharose Fast Flow column (2.5 × 30 cm; Amersham Pharmacia Biotech, Piscataway, NJ) equilibrated in the same buffer. Bound material was eluted with a 10 mM Na_2HPO_4/NaH_2PO_4, 100 mM NaCl buffer containing 50 mM imidazole. After exchange into 20 mM Na_2HPO_4/NaH_2PO_4 buffer, pH 7.8, active fractions were applied to an anion exchange Resource Q column (6 ml; Amersham Pharmacia Biotech) equilibrated with the same buffer. Bound fractions were eluted with a linear gradient of 200 mM to 1.0 M NaCl in Na_2HPO_4/NaH_2PO_4 buffer, pH 6.25. Active fractions were adjusted to 1.2 M $(NH_4)_2SO_4$, and applied to Macro-Prep Methyl Hydrophobic Interaction Chromatography column (2.5 × 30 cm; Bio-Rad Laboratories, Hercules, CA) equilibrated with 20 mM Na_2HPO_4/NaH_2PO_4 buffer containing 1.2 M $(NH_4)_2SO_4$, at pH 6.5. Bound material was eluted by a linear decreasing gradient of 1.2–0 M $(NH_4)_2SO_4$ in 20 mM Na_2HPO_4/NaH_2PO_4 buffer. Active fractions were loaded onto a Mini Q PC 3.2/3 anion exchange column (Amersham Pharmacia Biotech) equilibrated with 20 mM Na_2HPO_4/NaH_2PO_4 buffer, pH 7.8, and mounted on a Smart System (Amersham Pharmacia Biotech) equipped with a superloop. Bound material was eluted by a linear gradient of NaCl (20 mM to 1.0 M) in the starting buffer.

Cell Proliferation Assays. Fetal bovine heart endothelial cells (FBHE; American Type Culture Collection, Manassas, VA) were grown through passage 12 (14). Cells were trypsinized, washed, and cultured (800 cells/well in 0.2 ml DMEM culture medium with 10% heat inactivated FCS and 5 μg/ml gentamicin) for 5 d. DNA synthesis was measured by [^{3}H]thymidine deoxyribose uptake (0.5 mCi/well, 6.7 Ci/mmol; New England Nuclear, Boston, MA) during the last 20–23 h of culture. Human umbilical vein endothelial cells (HUVEC), prepared from umbilical cord by 0.1% collagenase II (Worthington Biochemical Corp., Freehold, NJ) digestion, were grown through passage 5, as described previously (25). Endothelial cell purity was >95%, as assessed by staining with a rabbit antiserum to human Factor VIII–related antigen (DAKO Corp., Carpinteria, CA). Cells were trypsinized (Trypsin/EDTA; GIBCO BRL), washed, and cultured in triplicate for 3 d (3.5×10^3 cells/well in 0.2 ml RPMI 1640 culture medium with 18% heat-inactivated FCS and 18 U/ml porcine heparin). Proliferation was measured by [^{3}H]thymidine uptake during the last 20–23 h of culture. Human mononuclear cells and mononuclear cells enriched for T or B lymphocytes were used in proliferation assays in the presence of phytohemagglutinin (Sigma Chemical Co.), pokeweed-mitogen (Sigma Chemical Co.), or EBV (B95-8 strain), as described previously (26). Conditions for proliferation (culture medium, cell density, length of culture) were optimized for each cell line, including: lymphoblastoid VDS-O (27); Burkitt lymphoma CA46, BL-41, KK124, Ag876, SHO (28); prostate adenocarcinoma TSU-Pr1 (from A. Passaniti, National Institutes of Health, Baltimore, MD); T cell Molt-4; Hodgkin's lymphoma Hs445; prostate adenocarcinoma Du145, and PC3; acute promyelocytic leukemia HL-60; neuroblastoma SKNMC; lung adenocarcinoma A549; breast adenocarcinoma MDA-MB-468; Wilms' tumor SK-NEP-1; colon carcinoma SW480; melanoma A-375; and human foreskin fibroblasts (H5 68) (all from American Type Culture Collection).

Two-dimensional Gel Electrophoresis, SDS-PAGE, and Western Blotting. Two-dimensional PAGE was performed as described previously (29). For SDS-PAGE and Western blot analysis, protein was solubilized in tricine SDS sample buffer (Novex, San Diego, CA), boiled, and run through 10–20% tricine gels. Gels were stained with Colloidal Coomassie G-250 stain or silver stain (Novex). Protein was transferred from gel onto Immobilon-P membranes (Millipore Corp., Bedford, MA). Membranes were incubated overnight with a rabbit anti–human calreticulin antiserum (Affinity Bioreagents Inc., Golden, CO), a rabbit anti–calreticulin N, or a rabbit anti–calreticulin P domain antiserum (30). Bound antibody was detected with an affinity-purified, peroxidase-linked, donkey anti–rabbit IgG antibody (Amersham Pharmacia Biotech), and a chemiluminescence detection system (ECL kit; Amersham Pharmacia Biotech).

Protein Sequencing. Protein spots were excised from the Coomassie-stained gel and destained. The proteins were digested with trypsin (Promega Corp., Madison, WI) in the gel (31), and the resulting fragments were separated by microcapillary HPLC and analyzed in-line by ion-trap mass spectrometry (model LCQ; Finnigan Corp., San Jose, CA) (32).

Matrigel Angiogenesis Assay. The Matrigel assay was performed as described previously (14). An aliquot (0.5 ml) of Matrigel (Becton Dickinson Labware, Bedford, MA), either alone or with desired additives, was injected subcutaneously into the midabdominal region of female BALB/c nude 6–8-wk-old mice. Five mice were injected with each mixture. After 5–7 d, the animals were killed and the Matrigel plugs were removed, fixed in 10% neutral buffered formalin solution (Sigma Chemical Co.), and embedded in paraffin. Tissues were sectioned (5-μm thickness), and slides were stained with Masson's trichrome. Quantitative analysis of angiogenesis in Matrigel plugs used a computerized semiautomated digital analyzer (model 40-10; Optomax, Hollis, NH). The average area occupied by cells/1.26×10^5 mm^2 Matrigel field was calculated. Results are expressed as the mean area occupied by cells per Matrigel field.

Production of Recombinant Calreticulin and Recombinant Vasostatin. The expression of the NH_2-terminal domain of human calreticulin fused to maltose-binding protein (MBP) in *Escherichia coli* was reported (33). The induction and purification of the fusion protein and MBP were accomplished according to New England Biolabs Inc. (Beverly, MA) protocols. Separation of MBP from vasostatin was accomplished by cleavage with Factor Xa, as described previously (33). Cleaved vasostatin was purified from MBP by anion exchange chromatography using a preequilibrated (20 mM Tris, pH 8.0, 25 mM NaCl) Resource Q column (Amersham Pharmacia Biotech), and elution by a stepwise gradient during which MBP eluted at 100–150 mM NaCl and calreticulin or vasostatin eluted at ~250 mM NaCl. We have produced 18 lots of vasostatin with consistent yields of highly purified protein, with comparable levels of biological activity as assessed by endothelial cell growth assays. All protein lots for in vivo and in vitro experiments (MBP-vasostatin, MBP, and cleaved vasostatin) were tested for endotoxin by the Limulus Amebocyte Lysate kinetic-QCL™ assay (BioWhittaker, Walkersville, MD) and were found to contain <5 EU/10 μg protein.

Mouse Tumor Models. BALB/c nu/nu female 6-wk-old mice (National Cancer Institute, Frederick, MD), maintained in pathogen-limited conditions, received 400 rad (1 rad = 0.01 Gy) total body irradiation and 24 h later were injected subcutaneously in the right abdominal quadrant with exponentially growing human

Burkitt lymphoma cells (10^7 CA46 cells; 15) or human colon carcinoma cell line (6×10^6 SW-480 cells; American Type Culture Collection) in 0.2 ml RPMI 1640 medium. In experiments designed to test tumor prevention, immediately after the cells were inoculated subcutaneously and continuing daily thereafter 6 d/wk, the mice received subcutaneous injections proximal to the site of original cell inoculation of test drug or appropriate controls. Formulation buffer consisted of sterile saline solution containing 50 mg/ml human albumin and 5 mg/ml mannitol (endotoxin <5 EU/ml). In experiments designed to evaluate effects on established tumors, cells were inoculated subcutaneously as described above, and the animals were observed until a tumor appeared. Beginning at this time, and continuing daily thereafter 6 d/wk, the mice received subcutaneous injections of test drug or appropriate controls proximal to the site of original cell inoculation. Tumor size was estimated (in cm^2) twice weekly as the product of two-dimensional caliper measurements (longest perpendicular length and width). A subcutaneous mass appearing at or proximal to the site of cell inoculation was considered a tumor when it measured at least 0.16 cm^2 in surface area and increased in size by at least 0.1 cm^2 over the following week.

Histology. Tumors and Matrigel plugs were fixed in 10% neutral buffered formalin solution (Sigma Chemical Co.), embedded in paraffin, sectioned at 4 μm, and stained with hematoxylin and eosin, or Masson's trichrome by standard methods.

Statistical Analysis. Student's *t* test was used to evaluate the significance of group differences; χ^2 analysis of 2×2 contingency table and Fisher's exact test were used to evaluate probability of association; Wilcoxon rank sums test was used to evaluate differences in tumor growth curves.

Results

Culture supernatants of an EBV-immortalized B cell line, VDS-O, profoundly inhibited the proliferation of primary HUVEC and FBHE induced by basic fibroblast growth factor (bFGF) (not shown). Using inhibition of bFGF-induced endothelial cell proliferation as an assay to monitor recovery of activity, we purified the inhibitory compounds from serum-free culture supernatants of the VDS-O cell line. The biologically active material was analyzed by two-dimensional gel electrophoresis under reduced conditions (Fig. 1). Two well-defined polypeptide spots were identified with molecular masses of ~55 and ~20 kD, and apparent isoelectric point of 4.7 and 5.6, respectively. A series of poorly defined spots with relative molecular masses ranging between 30 and 40 kD were also identified. The well-defined spots were trypsin digested and the tryptic fragments were analyzed by ion-trap mass spectrometry. By this method, the 55-kD polypeptide was identified as human calreticulin, and the 20-kD polypeptide as the light chain of human ferritin.

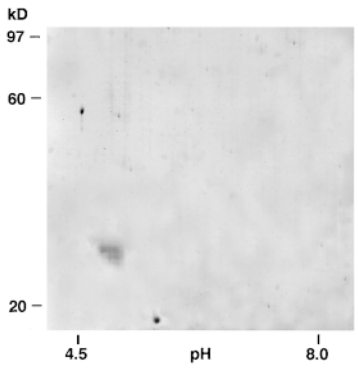

Figure 1. Two dimensional gel electrophoresis of purified material.

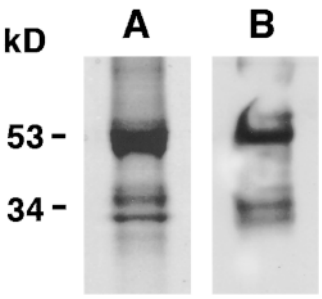

Figure 2. PAGE and Western blotting of purified cell line supernatant. Purified material was electrophoresed on a tricine gel containing 10–20% acrylamide. After electrophoresis, one lane (lane *A*) was stained with Colloidal Coomassie, and the other (lane *B*) was blotted onto transfer membrane and reacted overnight with a rabbit anti–human calreticulin antiserum (antibody PA3-900). Bound antibody was detected with an affinity-purified, peroxidase-linked, donkey anti–rabbit IgG antibody and a chemiluminescence detection system.

A rabbit antiserum to purified recombinant human calreticulin recognized the 55-kD component in a protein gel blot (Fig. 2 *A*, SDS-PAGE; Fig. 2 *B*, immunoblot). It also recognized the 30–40-kD bands, suggesting that they represent fragments of calreticulin. Antisera for human calreticulin NH_2-terminal (amino acids [aa] 6–19) and COOH-terminal (aa 382–400) peptides (30) identified the 55-kD band, confirming its identity to calreticulin. However, only the antiserum to the NH_2-terminal calreticulin peptide reacted with the 30–40-kD bands (not shown). We concluded that the biologically active, purified material contained human calreticulin, NH_2-terminal fragments of calreticulin, and the light chain of human ferritin.

To assess whether specific fragments of calreticulin might exhibit inhibitory activity, the NH_2-terminal calreticulin domain, which includes aa 1–180, was produced in *E. coli* as a fusion protein of MBP (MBP-calreticulin-N, 33). The purified MBP-calreticulin-N (Fig. 3, lane *2*) and the cleaved calreticulin-N (Fig. 3, lane *3*), but not control MBP (Fig. 3, lane *1*), inhibited the proliferation of FBHE (Fig. 4 and Table 1) and HUVEC (Table 1). We have named this calreticulin fragment (aa 1–180) vasostatin.

At concentrations of 0.5–2.5 μg/ml, vasostatin had minimal effect on: the proliferation of human PBMCs either unstimulated or stimulated with phytohemagglutinin; B and T cell–enriched peripheral blood cells stimulated with EBV and pokeweed mitogen, respectively; human foreskin fibroblasts (H568); Burkitt lymphoma cells; lymphoblastoid cells; T cells; neuroblastoma cells (SK-N-MC); lung carcinoma cells (A-549); breast adenocarcinoma cells (MDA-MB-468); acute promyelocytic leukemia cells (HL-60); prostate adenocarcinoma cells (Tsu-Pr1, PC-3, Dul45); Hodgkin's lymphoma cells (Hs445); colon adenocarcinoma cells (SW-480); Wilms' tumor cells (SK-NEP-1); and melanoma cells (A-375) (not shown).

The murine Matrigel assay (14) was used to evaluate the

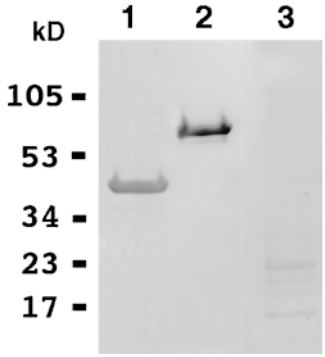

Figure 3. PAGE of recombinant purified proteins (lane *1*, MBP; lane *2*, MBP-vasostatin [calreticulin N-domain]; lane *3*, vasostatin). Recombinant MBP and MBP-vasostatin were purified as described. Separation of MBP from vasostatin was accomplished by cleavage with Factor Xa. Cleaved vasostatin was separated from MBP by anion exchange chromatography. Purified proteins were analyzed by electrophoresis on a 10–20% tricine gel and stained with Colloidal Coomassie G-250.

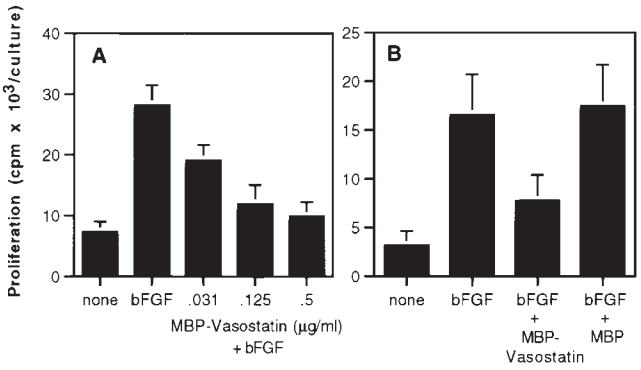

Figure 4. Inhibition of FBHE proliferation by MBP-vasostatin (calreticulin N-domain). FBHE were grown through passage 12. Cells were trypsinized, washed, and cultured (800 cells/well in 0.2 ml DMEM culture medium with 10% heat-inactivated FCS and 5 μg/ml gentamicin) for 5 d with or without bFGF (25 ng/ml). DNA synthesis was measured by [^{3}H]thymidine deoxyribose uptake during the last 20–23 h of culture. (*A*) Dose dependency of MBP-vasostatin inhibition. (*B*) Effects of 1 μg/ml MBP-vasostatin and MBP (average results of nine experiments).

effects of vasostatin on angiogenesis in vivo. When added to Matrigel at concentrations of 5–10 μg/ml, MBP-vasostatin and vasostatin (cleaved and purified from MBP-vasostatin) inhibited bFGF-induced neovascularization (Table 2).

Vasostatin was first tested for its ability to prevent growth of human Burkitt lymphomas in athymic mice. In a representative experiment (of three performed), MBP-vasostatin was injected for 18 d, at which time all animals with tumors were killed. The remaining mice continued treatment until tumor formation (Fig. 5 *A*). By day 18, 4 of 12 animals treated with MBP-vasostatin (60 μg/mouse) as opposed to 12 of 12 control-treated animals had developed a tumor ($P = 0.0013$). The mean (±SD) weight of tumors in the control group (0.43 ± 0.2 g) was greater than the weight of tumors from vasostatin-treated animals (0.21 ± 0.05 g), but the difference did not reach statistical significance ($P = 0.059$). With continued treatment, three additional tumors appeared on days 23, 64, and 91, but the remaining five animals remained tumor free as of day 160. We then compared the effects of vasostatin at two doses, 20 and 100 μg/mouse (Fig. 5 *B*). After 18 d of treatment, none of the mice (0 of 9) inoculated with MBP-vasostatin at the dose of 100 μg per mouse had developed a tumor. All (6 of 6) mice inoculated with buffer alone ($P = 0.0002$) and 3 of 5 mice inoculated with MBP-vasostatin at the dose of 20 μg/mouse developed a tumor (not significantly different from control, $P = 0.018$), indicating a dose effect. Treatment was continued unchanged until tumors appeared. As of day 44, only two tumors had appeared in the group treated with the highest dose.

We tested the effects of vasostatin on established human colon carcinoma and Burkitt lymphoma. The rate of colon carcinoma growth was significantly reduced in the group treated with vasostatin at a dose of 100 μg/mouse (12 mice) compared with the control group (10 mice) treated with formulation buffer alone ($P = 0.0003$, Fig. 5 *C*). All tumors were removed on day 39 of treatment. The mean (±SD) weight of colon carcinoma tumors in the control group (3.04 ± 0.6 g) was significantly ($P = 0.0004$) greater than the weight of tumors from vasostatin-treated animals (1.48 ± 0.64 g). In another experiment, the rate of Burkitt lymphoma growth (Fig. 5 *D*) was also significantly reduced in the group (9 mice) treated with vasostatin at a dose 200 μg/mouse compared with the controls (10 mice) treated with formulation buffer alone or MBP ($P = 0.003$). Tumors were removed on day 48. The mean weight of Burkitt tumors in the control group (6.89 ± 2.6 g) was significantly greater ($P = 0.0005$) than the mean weight of tumors treated with vasostatin (2.74 ± 0.6 g). There was no evidence of local or systemic toxicity in vasostatin-treated animals.

Table 1. *Inhibition of Endothelial Cell Proliferation by Vasostatin*

Additions to culture	Proliferation	Inhibition
	mean cpm/culture	*%*
*None	142	
bFGF	32,493	
MBP-vasostatin	17,930	44.8
MBP	34,363	
Vasostatin	13,231	59.3
‡None	4,210	
bFGF	28,050	
Vasostatin	9,864	64.8

HUVEC or FBHE were cultured in medium alone or in medium supplemented with bFGF (25 ng/ml). Recombinant purified MBP-vasostatin (1 μg/ml), vasostatin (1 μg/ml), or MBP (1 μg/ml) were added to cultures.

*Cultures containing HUVEC. HUVEC prepared from umbilical cord by 0.1% collagenase II digestion, were grown through passage 5. Endothelial cell purity was >95%, as assessed by staining with a rabbit antiserum to human Factor VIII–related antigen. Cells were trypsinized, washed, and cultured in triplicate for 3 d (3.5×10^3 cells/well in 0.2 ml RPMI 1640 culture medium with 18% heat-inactivated FCS and 18 U/ml porcine heparin). Proliferation was measured by [^{3}H]thymidine uptake during the last 20–23 h of culture. The results reflect the mean of triplicate cultures; SDs are within 10% of the mean. Results are representative of five experiments performed.

‡Cultures containing FBHE, as described in the legend to Fig. 3. The results reflect the mean of three experiments.

Table 2. *Effects of Vasostatin on Angiogenesis In Vivo*

Additions to Matrigel	Mean surface area occupied by cells	Inhibition
	$mm^2/1.26 \times 10^5\ mm^2$	%
None	649	
bFGF	11,544	
bFGF + MBP-vasostatin (10 μg/ml)	4,539	61
bFGF + MBP-vasostatin (5 μg/ml)	5,286	54
bFGF + MBP (10 μg/ml)	9,186	20
None	487	
bFGF	14,472	
bFGF + MBP-vasostatin (5 μg/ml)	4,989	66
bFGF + vasostatin (5 μg/ml)	4,638	68
MBP (5 μg/ml)	13,472	7

Mice (BALB/c nude, 6–8-wk-old, five mice per group) were injected subcutaneously into the midabdominal region with Matrigel alone; Matrigel plus bFGF; or Matrigel plus bFGF (150 ng/ml) plus MBP-vasostatin, MBP, or vasostatin (in all cases, total injection volume 0.5 ml). Plugs were removed after 5–7 d, fixed in 10% neutral buffered formalin solution, embedded in paraffin, and histologic sections were stained with Masson's trichrome. The results reflect the mean surface area (expressed in mm^2) occupied by cells within a circular surface area of 1.26×10^5 mm^2. All lots of MBP and MBP-vasostatin contained <5 U endotoxin/10 μg protein as determined by the Limulus Amebocyte Lysate assay.

Histology showed that tissue from control tumors and tumors treated with vasostatin were indistinguishable with respect to morphology of tumor cells and the number of mitoses. However, vasostatin-treated tumors occasionally displayed changes in the tumor vasculature, including intimal and medial thickening, focal fibrinoid necrosis of the vessel wall, and occasional infiltration with neutrophils, histiocytes, and lymphocytes (Fig. 5, *E* and *F*). These alterations were absent from parallel tumors of control animals. No abnormalities were noted on gross and histological examination of liver, spleen, kidneys, heart, lung, and lymph nodes from vasostatin-treated animals.

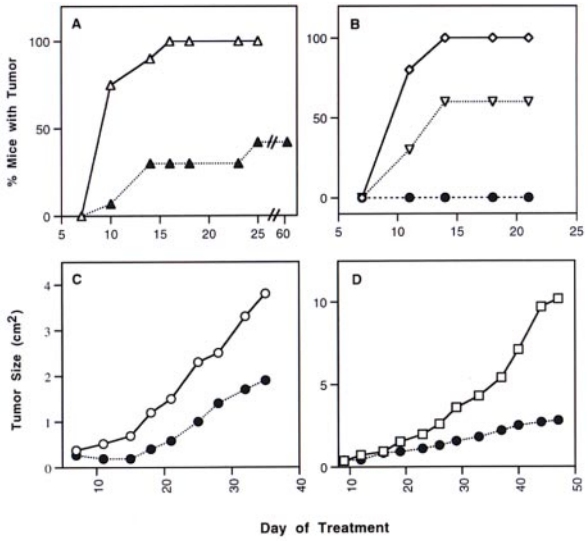

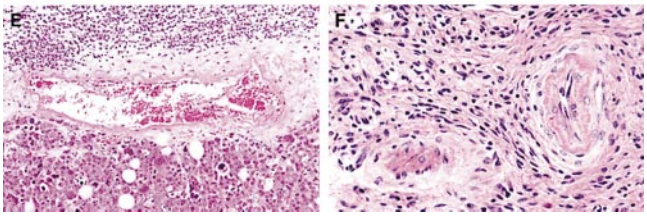

Figure 5. Inhibition of tumor growth by vasostatin. Burkitt lymphoma cells (CA46 cell line, 10^7 cells in 0.2 ml RPMI 1640 medium) were inoculated subcutaneously into BALB/c athymic mice, 6 wk old. Beginning on the day of cell inoculation and continuing thereafter daily (6 d/wk), mice were inoculated subcutaneously proximal to the site of cell inoculation with either formulation buffer (sterile water containing 0.5% mannitol, 5% human albumin, and 1% sodium chloride) or test protein (*A* and *B*). (*A*) 12 mice were inoculated with control purified MBP (40 μg/d × 18 d), and 12 mice were inoculated with MBP-vasostatin (60 μg/day × 18 d); all mice with tumor (12 treated with MBP and 4 treated with MBP-vasostatin) were killed on day 18. The remaining mice were observed. (*B*) Six mice were treated with formulation buffer alone (0.1 ml/d × 22 d), five mice were treated with 20 μg/d × 22 d purified MBP-vasostatin (open triangle), and nine mice were treated with 100 μg/d × 22 d purified MBP-vasostatin (filled circle). (*C*) Mice (BALB/c athymic mice, 6 wk old) were inoculated subcutaneously with the human colon carcinoma cell line (SW-480, 6×10^6 cells/mouse in 0.2 ml RPMI medium). After a tumor appeared (at least 130 mm^2 in size), 12 mice were treated with MBP-vasostatin (100 μg/d, 6 d/wk, 100 μl/dose, × 36 d), and 10 mice were inoculated with formulation buffer (100 μl × 36 d). Tumor size was estimated as the product of two-dimensional caliper measurements. (*D*) Mice were inoculated subcutaneously with the human Burkitt lymphoma cell line CA46 as described above. After a tumor appeared (at least 130 mm^2 in size), 9 mice were treated with MBP-vasostatin (200 μg/d, 6 d/wk, 100 μl/dose × 46 d) and 10 mice were treated with formulation buffer alone (100 μl × 46 d). (*E* and *F*) Histology of Burkitt tumors after treatment with MBP-vasostatin depicting a characteristic vessel with fibrinoid necrosis and surrounding neutrophil infiltration (*E*), and a vessel with intimal and medial thickening (*F*); Hematoxylin-eosin stain; ×63.

Discussion

These results show that vasostatin, an NH_2-terminal fragment of human calreticulin, can inhibit endothelial cell proliferation in vitro, suppress neovascularization in vivo, and prevent or reduce growth of experimental tumors. Calreticulin, a ubiquitous and highly conserved protein originally identified in skeletal muscle sarcoplasmic reticulum, serves as one of the major storage depots for calcium ions within the endoplasmic reticulum and participates in calcium signaling (34–36). The NH_2-domain of calreticulin, which includes aa 1–180, is the most conserved domain among the calreticulins so far cloned and has no homology to other protein sequences (34, 35). Although it does not bind calcium, it can bind the cytoplasmic domain of α subunits of integrins regulating cell attachment (37), can inter-

act with the nuclear receptors for glucocorticoid, androgen, and retinoic acid, regulating their binding to DNA (38), and can, once phosphorylated, bind stem-loop structures at the 3′-end of rubella virus genomic RNA contributing to virus replication (30, 33). However, neither calreticulin nor the NH_2-domain of calreticulin has been shown previously to inhibit endothelial cell growth, angiogenesis, or tumor growth.

Vasostatin directly and specifically inhibited endothelial cell growth but had minimal effect on the growth of other cells. Previously, calreticulin was reported to bind specifically and reversibly to endothelial cells in vitro with a K_d of ~7.4 nM, and to localize selectively to the vascular endothelium in vivo. It was also found to promote nitric oxide release from endothelial cells (39). Although its role in angiogenesis is controversial, nitric oxide was reported to suppress angiogenesis and endothelial cell migration (40, 41). We do not know the mechanism by which vasostatin inhibits endothelial cell growth. Preliminary experiments in vitro have failed to support a role of nitric oxide as a mediator of growth inhibition by vasostatin. However, we believe that inhibition of endothelial cell proliferation is central to suppression of angiogenesis and tumor growth by vasostatin. In the Matrigel angiogenesis assay, plugs with vasostatin contained significantly fewer endothelial cells compared with control plugs. In vitro, tumor cells were not growth inhibited by vasostatin, and in vivo, tumor tissues from vasostatin-treated mice were histologically similar to controls, suggesting that vasostatin acts indirectly on tumor cells. In vasostatin-treated animals, vessels distant from the tumor appeared normal, and even the established tumor vasculature had limited evidence of vasostatin-induced damage. This suggests that the antitumor effects of vasostatin are related to inhibition of new vessel formation rather than to a toxic effect on established tumor vascular structures.

Tumor regression induced by EBV-immortalized cells is characterized by reduced tumor growth, extensive tumor tissue necrosis leading to complete tumor regression, and vascular damage (17, 23, 24). The chemokines IP-10 and Mig, induced but not secreted by EBV-immortalized cells, contributed to tumor regression in this model by promoting extensive tumor tissue necrosis and intravascular thrombosis (15, 17). Exogenous IL-12 exerted similar effects due to its induction of IP-10 and Mig (42, 43). However, IP-10 and Mig treatment minimally reduced tumor size, and tumors eventually grew (15, 17). We now show that vasostatin significantly reduced tumor growth without causing tumor tissue necrosis or extensive intravascular thrombosis. Therefore, it will be interesting to test the antitumor effects of vasostatin treatment combined with IP-10, Mig, or IL-12.

A number of favorable features set vasostatin apart from other inhibitors of angiogenesis. Compared with thrombospondin, angiostatin and endostatin, vasostatin is a small, soluble, and stable molecule that is easy to produce and deliver. We have produced 18 independent batches of recombinant vasostatin, with consistent yields of biologically active, purified protein that were stable for >9 mo in aqueous solution. By contrast, endostatin produced in *E. coli* was insoluble, and was thus used as a suspension for in vivo studies (11). Angiostatin was produced by proteolysis of human plasminogen purified from plasma (10). Thrombospondin was purified from human platelets (44). Thus, unlike vasostatin, these molecules may represent manufacturing challenges. In addition, the effective dose of vasostatin in mice was 4–10-fold lower than the effective doses of endostatin or angiostatin (10, 11). Thrombospondin, inhibitory at nanomolar concentrations, promotes endothelial cell migration at higher concentrations (45). A requirement for large drug doses or complex dose–function relationships may add cost and challenges to product development. Furthermore, although vasostatin specifically targeted proliferating endothelial cells, other inhibitors such as thrombospondin appear to have more complex activities (44). Angiostatin and endostatin may not only inhibit proliferating endothelial cells, but may also be toxic for the established tumor vasculature (46).

As yet, we do not know the full spectrum of tumors that are responsive to the angiostatic effects of vasostatin, the optimal vasostatin dose and regimen, or whether spontaneous tumors in their natural sites are responsive to vasostatin. We report that vasostatin, the NH_2-domain of calreticulin, is a potent and selective endothelial cell growth inhibitor that suppresses angiogenesis and tumor growth. These results emphasize the potential benefits of drugs that target angiogenesis in the prevention and treatment of human cancer.

We thank Dan Bolling (Pharmacia, Piscataway, NJ) and Drs. M. Moos, E. Jaffe, C. Atreya, P. Duncan, G. Pogue, D. Garland, H. Kleinman, and R. Yarchoan.

Address correspondence to Giovanna Tosato, Center for Biologics Evaluation and Research, Building 29A, Room 2D16, HFM535, 1401 Rockville Pike, Rockville, MD 20852-1448. Phone: 301-827-1794; Fax: 301-480-3256; E-mail: Tosato@A1.CBER.FDA.GOV

Received for publication 2 September 1998.

References

1. Folkman, J. 1982. Angiogenesis: initiation and control. *Ann. NY Acad. Sci.* 401:212–227.
2. Hanahan, D., and J. Folkman. 1996. Patterns and emerging mechanisms of the angiogenic switch during tumorigenesis. *Cell.* 86:353–364.
3. Kim, K.J., B. Li, J. Winer, M. Armanini, N. Gillett, H.S. Phillips, and N. Ferrara. 1993. Inhibition of vascular endothelial growth factor–induced angiogenesis suppresses tumour

growth in vivo. *Nature*. 362:841–844.
4. Kendall, R.L., and K.A. Thomas. 1993. Inhibition of vascular endothelial cell growth factor activity by an endogenously encoded soluble receptor. *Proc. Natl. Acad. Sci. USA*. 90: 10705–10709.
5. Skobe, M., P. Rockwell, N. Goldstein, S. Vosseler, and N.E. Fusenig. 1997. Halting angiogenesis suppresses carcinoma cell invasion. *Nat. Med.* 3:1222–1227.
6. Cheresh, D.A., and R.C. Spiro. 1987. Biosynthetic and functional properties of an Arg-Gly-Asp–directed receptor involved in human melanoma cell attachment to vitronectin, fibrinogen, and von Willebrand factor. *J. Biol. Chem*. 262: 17703–17711.
7. Brooks, P., A. Clark, and D. Cheresh. 1994. Requirement of vascular integrin ab_3 for angiogenesis. *Science*. 264:569–571.
8. Brooks, P.C., A.M. Montgomery, M. Rosenfeld, R.A. Reisfeld, T. Hu, G. Klier, and D.A. Cheresh. 1994. Integrin α v β 3 antagonists promote tumor regression by inducing apoptosis of angiogenic blood vessels. *Cell*. 79:1157–1164.
9. O'Reilly, M.S., L. Holmgren, Y. Shing, C. Chen, R.A. Rosenthal, M. Moses, W.S. Lane, Y. Cao, E.H. Sage, and J. Folkman. 1994. Angiostatin: a novel angiogenesis inhibitor that mediates the suppression of metastases by a Lewis lung carcinoma. *Cell*. 79:315–328.
10. O'Reilly, M.S., L. Holmgren, C. Chen, and J. Folkman. 1996. Angiostatin induces and sustains dormancy of human primary tumors in mice. *Nat. Med*. 2:689–692.
11. O'Reilly, M.S., T. Boehm, Y. Shing, N. Fukai, G. Vasios, W.S. Lane, E. Flynn, J.R. Birkhead, B.R. Olsen, and J. Folkman. 1997. Endostatin: an endogenous inhibitor of angiogenesis and tumor growth. *Cell*. 88:277–285.
12. Boehm, T., J. Folkman, T. Browder, and M.S. O'Reilly. 1997. Antiangiogenic therapy of experimental cancer does not induce acquired drug resistance. *Nature*. 390:404–407.
13. Voest, E.E., B.M. Kenyon, M.S. O'Reilly, G. Truitt, R.J. D'Amato, and J. Folkman. 1995. Inhibition of angiogenesis in vivo by interleukin 12. *J. Natl. Cancer Inst.* 87:581–586.
14. Angiolillo, A.L., C. Sgadari, D.D. Taub, F. Liao, J.M. Farber, S. Maheshwari, H.K. Kleinman, G.H. Reaman, and G. Tosato. 1995. Human interferon–inducible protein 10 is a potent inhibitor of angiogenesis in vivo. *J. Exp. Med*. 182:155–162.
15. Sgadari, C., A.L. Angiolillo, B.W. Cherney, S.E. Pike, J.M. Farber, L.G. Koniaris, P. Vanguri, P.R. Burd, N. Sheikh, G. Gupta, et al. 1996. Interferon-inducible protein 10 identified as a mediator of tumor necrosis in vivo. *Proc. Natl. Acad. Sci. USA*. 93:13791–13796.
16. Strieter, R.M., S.L. Kunkel, D.A. Arenberg, M.D. Burdick, and P.J. Polverini. 1995. Interferon gamma–inducible protein 10 (IP-10), a member of the C-X-C chemokine family, is an inhibitor of angiogenesis. *Biochem. Biophys. Res. Commun*. 210:51–57.
17. Sgadari, C., J.M. Farber, A.L. Angiolillo, F. Liao, J. Teruya-Feldstein, P.R. Burd, L. Yao, G. Gupta, C. Kanegane, and G. Tosato. 1997. Mig, the monokine induced by interferon-gamma, promotes tumor necrosis in vivo. *Blood*. 89:2635–2643.
18. Clapp, C., J.A. Martial, R.C. Guzman, F. Rentier-Delure, and R.I. Weiner. 1993. The 16 kilodalton N-terminal fragment of human prolactin is a potent inhibitor of angiogenesis. *Endocrinology*. 133:1292–1299.
19. Ingber, D., T. Fujita, S. Kishimoto, K. Sudo, T. Kanamaru, H. Brem, and J. Folkman. 1990. Synthetic analogues of fumagillin that inhibit angiogenesis and suppress tumor growth. *Nature*. 348:555–557.
20. D'Amato, R.J., M.S. Loughnan, E. Flynn, and J. Folkman. 1994. Thalidomide is an inhibitor of angiogenesis. *Proc. Natl. Acad. Sci. USA*. 91:4082–4085.
21. Maione, T.E., G.S. Gray, J. Petro, A.J. Hunt, A.L. Donner, S.I. Bauer, H.F. Carson, and R.J. Sharpe. 1990. Inhibition of angiogenesis by recombinant human platelet factor–4 and related peptides. *Science*. 247:77–79.
22. Good, D.J., P.J. Polverini, F. Rastinejad, M.M. Le Beau, R.S. Lemons, W.A. Frazier, and N.P. Bouck. 1990. A tumor suppressor–dependent inhibitor of angiogenesis is immunologically and functionally indistinguishable from a fragment of thrombospondin. *Proc. Natl. Acad. Sci. USA*. 87:6624–6628.
23. Tosato, G., C. Sgadari, K. Taga, K.D. Jones, S.E. Pike, A. Rosenberg, J.M. Sechler, I.T. Magrath, L.A. Love, and K. Bhatia. 1994. Regression of experimental Burkitt's lymphoma induced by Epstein-Barr virus–immortalized human B cells. *Blood*. 83:776–784.
24. Angiolillo, A.L., C. Sgadari, N. Sheikh, G.H. Reaman, and G. Tosato. 1995. Regression of experimental human leukemias and solid tumors induced by Epstein-Barr virus–immortalized B cells. *Leuk. Lymphoma*. 19:267–276.
25. Gordon, P.B., I.I. Sussman, and V.B. Hatcher. 1983. Long-term culture of human endothelial cells. *In Vitro*. 19:661–671.
26. Tosato, G., T.L. Gerrard, N.G. Goldman, and S.E. Pike. 1988. Stimulation of EBV-activated human B cells by monocytes and monocyte products. Role of IFN-β 2/B cell stimulatory factor 2/IL-6. *J. Immunol.* 140:4329–4336.
27. Tosato, G., G.E. Marti, R. Yarchoan, C.A. Heilman, F. Wang, S.E. Pike, S.J. Korsmeyer, and K. Siminovitch. 1986. Epstein-Barr virus immortalization of normal cells of B cell lineage with nonproductive, rearranged immunoglobulin genes. *J. Immunol*. 137:2037–2042.
28. Cherney, B.W., K.G. Bhatia, C. Sgadari, M.I. Gutierrez, H. Mostowski, S.E. Pike, G. Gupta, I.T. Magrath, and G. Tosato. 1997. Role of the p53 tumor suppressor gene in the tumorigenicity of Burkitt's lymphoma cells. *Cancer Res*. 57: 2508–2515.
29. Wirth, P.J., T.N. Hoang, and T. Benjamin. 1995. Micropreparative immobilized pH gradient two-dimensional electrophoresis in combination with protein microsequencing for the analysis of human liver proteins. *Electrophoresis*. 16:1946–1960.
30. Pogue, G.P., X.Q. Cao, N.K. Singh, and H.L. Nakhasi. 1993. 5′ sequences of rubella virus RNA stimulate translation of chimeric RNAs and specifically interact with two host-encoded proteins. *J. Virol*. 67:7106–7117.
31. Li, G., M. Waltham, N.L. Anderson, E. Unsworth, A. Treston, and J.N. Weinstein. 1997. Rapid mass spectrometric identification of proteins from two-dimensional polyacrylamide gels after in gel proteolytic digestion. *Electrophoresis*. 18: 391–402.
32. Hunt, D.F., R.A. Henderson, J. Shabanowitz, K. Sakaguchi, H. Michel, N. Sevilir, A.L. Cox, E. Appella, and V.H. Engelhard. 1992. Characterization of peptides bound to the class I MHC molecule HLA-A2.1 by mass spectrometry. *Science*. 255:1261–1263.
33. Atreya, C.D., N.K. Singh, and H.L. Nakhasi. 1995. The rubella virus RNA binding activity of human calreticulin is localized to the N-terminal domain. *J. Virol*. 69:3848–3851.
34. Michalak, M., R.E. Milner, K. Burns, and M. Opas. 1992.

Calreticulin. *Biochem. J.* 285:681–692.
35. Nash, P.D., M. Opas, and M. Michalak. 1994. Calreticulin: not just another calcium-binding protein. *Mol. Cell. Biochem.* 135:71–78.
36. Krause, K.H., and M. Michalak. 1997. Calreticulin. *Cell.* 88: 439–443.
37. Coppolino, M.G., M.J. Woodside, N. Demaurex, S. Grinstein, R. St-Arnaud, and S. Dedhar. 1997. Calreticulin is essential for integrin-mediated calcium signalling and cell adhesion. *Nature.* 386:843–847.
38. Burns, K., B. Duggan, E.A. Atkinson, K.S. Famulski, M. Nemer, R.C. Bleackley, and M. Michalak. 1994. Modulation of gene expression by calreticulin binding to the glucocorticoid receptor. *Nature.* 367:476–480.
39. Kuwabara, K., D.J. Pinsky, A.M. Schmidt, C. Benedict, J. Brett, S. Ogawa, M.J. Broekman, A.J. Marcus, R.R. Sciacca, M. Michalak, et al. 1995. Calreticulin, an antithrombotic agent which binds to vitamin K-dependent coagulation factors, stimulates endothelial nitric oxide production, and limits thrombosis in canine coronary arteries. *J. Biol. Chem.* 270: 8179–8187.
40. Pipili-Synetos, E., E. Sakkoula, G. Haralabopoulos, P. Andriopoulou, P. Peristeris, and M.E. Maragoudakis. 1994. Evidence that nitric oxide is an endogenous antiangiogenic mediator. *Br. J. Pharmacol.* 111:894–902.
41. Lau, Y.T., and W.C. Ma. 1996. Nitric oxide inhibits migration of cultured endothelial cells. *Biochem. Biophys. Res. Commun.* 221:670–674.
42. Tannenbaum, C.S., R. Tubbs, D. Armstrong, J.H. Finke, R.M. Bukowski, and T.A. Hamilton. 1998. The CXC chemokines IP-10 and Mig are necessary for IL-12–mediated regression of the mouse RENCA tumor. *J. Immunol.* 161: 927–932.
43. Kanegane, C., C. Sgadari, H. Kanegane, J. Teruya-Feldstein, L. Yao, G. Gupta, and G. Tosato. 1998. Contribution of the CXC chemokines IP-10 and Mig to the antitumor effects of IL-12. *J. Leuko. Biol.* 64:384–392.
44. Volpert, O.V., J. Lawler, and N.P. Bouck. 1998. A human fibrosarcoma inhibits systemic angiogenesis and the growth of experimental metastases via thrombospondin-1. *Proc. Natl. Acad. Sci. USA.* 95:6343–6348.
45. Gao, A.G., F.P. Lindberg, M.B. Finn, S.D. Blystone, E.J. Brown, and W.A. Frazier. 1996. Integrin-associated protein is a receptor for the C-terminal domain of thrombospondin. *J. Biol. Chem.* 271:21–24.
46. Hanahan, D. 1998. A flanking attack on cancer. *Nat. Med.* 4:13–14.